High-pressure structural studies of MOH layered compounds (M=Na, K, Rb, Cs)

1995 J. Phys.: Condens. Matter 7 5461

(http://iopscience.iop.org/0953-8984/7/28/005)

J. Phys.: Condens. Matter 7 (1995) 5461–5476. Printed in the UK

High-pressure structural studies of MOH layered compounds (M = Na, K, Rb, Cs)

J W Otto† and W B Holzapfel
FB 6, Uni-GH Paderborn, D-33095 Paderborn, Germany

Received 17 November 1994, in final form 23 March 1995

Abstract. The structures of alkali metal (Na, K, Rb, Cs) hydroxides were investigated using energy-dispersive x-ray diffraction at pressures up to 20 GPa. The phase transitions previously discovered with optical methods (by Krobok and co-authors in 1992 and 1994) are confirmed. A structure is proposed for the high-pressure phases of KOH and RbOH, and for a predicted phase of CsOH. Equation of state parameters are presented for the phases encountered.

1. Introduction

Strongly ionic AB compounds crystallize in either the NaCl (six-coordinated) or CsCl (eight-coordinated) structure type depending on the radius ratio of cation to anion. When the anion is a non-spherical polar molecule (such as CN^- or OH^-), increasing distortions from the high-temperature disordered NaCl or CsCl structures are found with decreasing temperature. These distortions are sensitive to the details of the charge distribution (such as the polarity of the anion, the charge density of the cation and, in particular, to hydrogen bonding).

In the alkali metal hydroxides, a distinct series of phase transitions with decreasing temperature from disordered to distorted NaCl-type and then to TlI-type structures has been observed [3–6]. The first-order phase transitions in hydroxides are due to the freezing-out of the free or quasi-free rotations of OH^- groups. The increasing dipole character of the anion with decreasing temperature leads to a repulsion between the metal cation and the H^+ ion with the formation of metal–oxygen double layers. The double layers approach each other unless a high charge density on the cation causes strong metal–hydrogen repulsion (as in NaOH). On close approach of the layers, hydrogen bonds are formed building one-dimensional chains between the layers. The formation of the hydrogen bonds may be assisted by a shear of the layers until the interlayer distance is minimized while also minimizing the metal–hydrogen repulsion (as in KOH and RbOH). In CsOH, the intermediate distorted NaCl-type structure does not occur. Under pressure, the interlayer distances are expected to shorten drastically since the weak interlayer bonds (van der Waals and/or hydrogen bonds) are very compressible. This may lead to hydrogen bonding in NaOH and to a collapse of the layered phases towards the CsCl-type structures in the heavier alkali metal hydroxides. Recent Raman and infrared studies of these compounds at and below room temperature and at pressures up to 20 GPa have shown that, at low pressures, transitions to well-known low-temperature phases take place [1, 2]. At higher pressures, transitions to unknown structures were found in NaOH, KOH and RbOH. The

† Current address: HASYLAB, Notkestrasse 85, D-22603 Hamburg, Germany.

0953-8984/95/285461+16$19.50

present study was undertaken to determine the structures of these new phases and to confirm the presence of the low-temperature structures at intermediate pressures. The high-pressure structure of NaOH has recently been determined in an independent study [7].

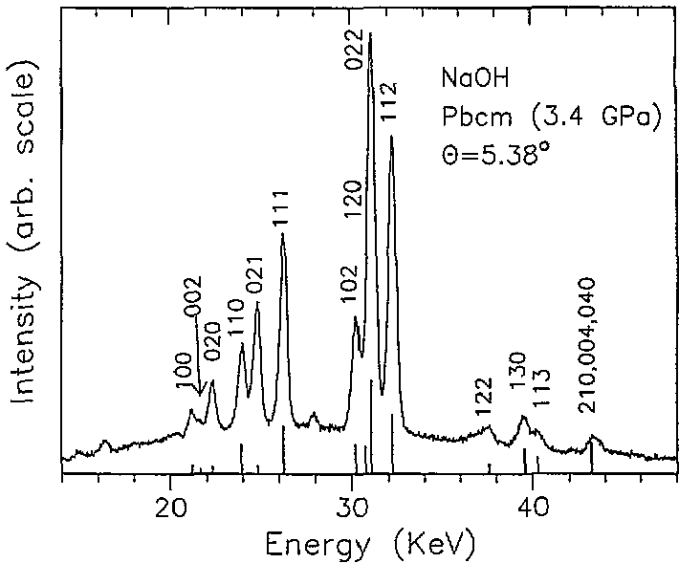

Figure 1. EDX spectrum of NaOH at 3.4 GPa. The pattern was indexed with the *Pbcm* structure determined previously [7]. The small peak at around 28 keV is the (111) reflection of the *Cmcm* (ambient pressure) structure. The intensities (shown by the vertical bars) were calculated for EDX with synchrotron using the ENDIX program [18].

2. Experimental details

NaOH (semiconductor-grade pellets, Aldrich Chemicals) and KOH ('ultrapure', Johnson–Matthey Alfa Products) were dried as previously described [1]. RbOH and CsOH were synthesized by H Barlage using the methods previously described [5–8]. The samples were sealed in quartz ampoules under an argon atmosphere. For the high-pressure experiments, the ampoules were opened under mineral or paraffin oil and the material was syphoned off. In the case of the most reactive hydroxides (RbOH and CsOH), the oil had been dried with pieces of potassium. The samples were not ground prior to the experiments although the grain size was rather large ($\geqslant$30 μm in the case of CsOH). In general, many trial fillings of the gasket hole were necessary to obtain a sample without a strong texture, indicating that the size of the crystals within individual grains was also rather large. Apparently, the only fillings that were successful were those in which there was either a favourable distribution of crystals from the start or in which the grains were crushed during the closing of the cell or the low-pressure phase transitions. Contamination by black particles from the externally heated pressure vessel in which the samples had been prepared was present in the ampoules of CsOH and RbOH. Additional peaks present in the spectra of the second runs on RbOH and CsOH show that some of this material apparently contaminated the sample in the pressure cell. However, the results of the different experiments were consistent. After filling, the cell was closed immediately to above 1 GPa to avoid reaction with H_2O or CO_2. Therefore, spectra at ambient conditions were obtained only on pressure release. For the experiments, a diamond-anvil cell [9] was used equipped with inconel gaskets 70 to 80

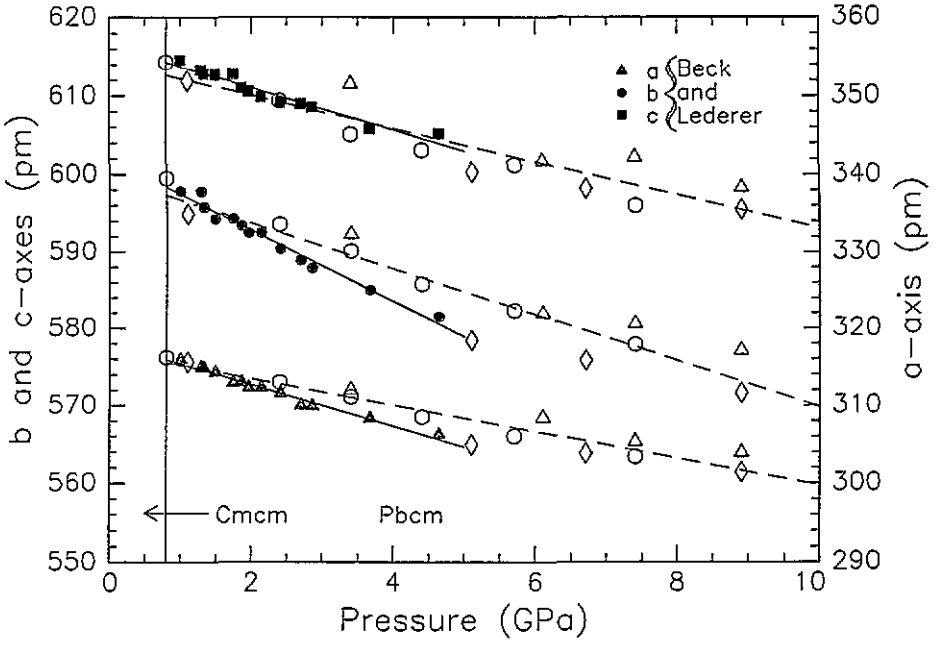

Figure 2. Lattice parameters of NaOH in the *Pbcm* structure versus pressure. The data of [7] are shown by the solid symbols. The open symbols refer to the different runs performed in the present study. The solid and dashed lines are fits to the data of [7] and to the present results, respectively.

μm thick with holes of 240 μm in diameter. For measuring the pressure with the ruby fluorescence method [10], small grains of ruby (approximately 5×5 μm) were attached to the piston diamond with apiezon grease.

The experiments were performed with energy-dispersive x-ray diffraction (EDX) at HASYLAB [11] using the set-up previously described [12]. A W–Ni crossed slit with variable openings in the range 100×100 μm to 140×140 μm was used to collimate the beam. Two vertical Ta slits of 100 and 120 μm spaced 40 cm apart were placed in the diffracted beam between the sample and the detector. Several runs were performed for each compound, at 4.60°, 5.09° and 5.38° for NaOH, 5.38° and 3.67° for KOH, 5.38° (3.59° during de-pressurization) and 5.30° for RbOH, and 4.95° and 5.31° for CsOH.

All metal hydroxides investigated here turned a purple or brownish colour after long irradiation in the x-ray beam due to generation of colour centres. The colour centres remained after releasing the pressure; the samples begin to melt on opening the cell due to the take-up of CO_2 and H_2O and no studies of possible bleaching were performed. The experiments were performed at HASYLAB with DORIS running at 4.46 GeV. Currents were typically in the range 80–40 mA. The x-ray intensities for the known and proposed structures were calculated for the energy-dispersive case in the Debye–Scherrer geometry using the ENDIX program [18]. This program calculates the integrated intensity for a powder in the kinematic approximation with an approximation for the correction of the detector efficiency, intensity distribution of the synchrotron and various experimental parameters (such as the absorption due to the diamonds and the scattering in air).

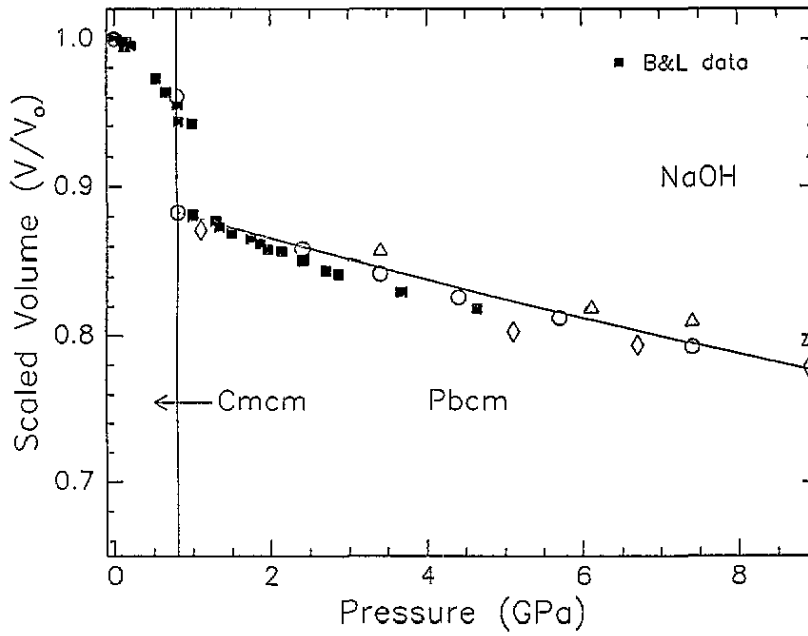

Figure 3. Scaled volume of NaOH versus pressure. The data of [7] are indicated by the solid symbols. The present data (shown by the open symbols) were fitted assuming that the run at 0.8 GPa determines the volume at the phase transition.

3. Results

3.1. NaOH

A phase transition from the room temperature structure (space group *Cmcm*) with a volume change of 7.8% had previously been identified at 0.84 GPa in DTA measurements [13]. Raman and infrared studies showed that (a) the number of atoms per primitive unit cell remains unchanged in that transition (there is no change in the number of fundamental modes) and (b) the high-pressure phase does not have linear hydrogen bonds, although bent or bifurcated hydrogen bonds cannot be excluded (there is little change in the frequency of the stretching mode with pressure) [1]. The transition pressure was found to be in the range 0.8–1.0 GPa. An angle-dispersive x-ray diffraction study confirmed the transition pressure of 1 GPa, and determined a distorted NiAs-type structure (space group *Pbcm*) [7]. The hydrogen atoms could not be located in that study.

The lattice parameters determined for the *Cmcm* structure at ambient conditions in the present study are in reasonable agreement with the literature values (see table 1). Coexistence of two phases was found in a run at 0.8 GPa, from which an upper limit of 9.2% volume change at the phase transition was calculated; this is to be compared with a change of 6.6% determined by [7]. The high-pressure structure was indexed with the *Pbcm* space group determined by [7] (figure 1). This structure was found to be stable to at least 20 GPa. However, lattice constants could be determined only up to 10 GPa because of peak overlap and the development of a strong texture. At high pressures, only peaks with (0*kl*) indices were observed, showing that the shortest axis (the *a*-axis) tends to orient along the axis of compression. The compression of all three axes was found to be linear, although the scatter of the data from the different experiments is quite large (figure 2).

Table 1. Lattice parameters for the ambient-pressure phases and equation of state parameters for the intermediate- and high-pressure phases. V_0 (the molar volume at ambient pressure) and K_0 were calculated for a first-order Birch equation of state [14]. Literature values for the lattice parameters of the ambient-pressure phases are from [3] (NaOH and KOH), [5] (RbOH) and [8] (CsOH). Lattice parameters are in pm, and bulk moduli in GPa. The errors indicated in brackets are the statistical errors of the fitting procedures only and do not reflect the experimental errors.

		NaOH		KOH		RbOH		CsOH	
Phase	Parameter	This work	Literature	This work	Literature	This work	Literature	This work	Literature
Ambient pressure	a	340.4(1)	340.13(4)	397.1	395.7(5)	415.0	414.70(7)	435.3(1)	435.0(3)
	b	1138.2(2)	1137.88(3)	399.6	399.5(1)	423.2	423.03(5)	1203.2(2)	1199.2(8)
	c	340.5(1)	338.3(2)	576.4	574.2(2)	601.2	600.5(1)	452.2(1)	451.6(3)
	β	—	—	103.54°	103.93(8)°	105.44°	105.38(2)°	—	—
Inter-mediate pressure	V_0 $\times 10^6$	—	—	43.3 (0.7)	—	49.2 (0.7)	—	56.4 (0.4)	—
	K_0	—	—	24.5 (3.8)	—	23.2 (3.0)	—	29.7 (1.5)	—
High pressure (*Pbcm*)	V_0 $\times 10^6$	29.7 (0.4)	29.7 (0.1)†	46.8 (0.9)	—	44.92 (1.9)	—	—	—
	K_0	45.9 (6.3)	37.2 (1.3)†	56.8 (11.6)	—	33.6 (10.1)	—	—	—

† *Calculated from* [7].

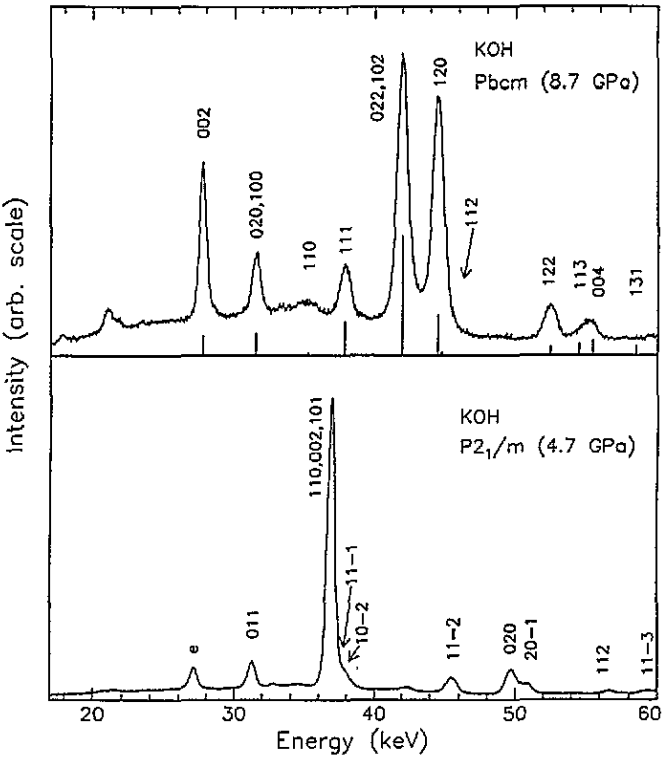

Figure 4. EDX spectra of KOH at 4.7 GPa ($P2_1/m$ structure, bottom) and at 8.7 GPa (orthorhombic structure, top) at an angle of 3.67°. The high-pressure structure was fitted with an orthorhombic space group. The indexing and calculated intensities for an anti-NaOH structure in the *Pbcm* space group are shown as an example.

The lattice constants and the volume determined close to the transition pressure agree well with the values determined by [7] (figures 2 and 3). The compressibilities of the a- and b-axes, however, were found to be smaller than those determined by [7]. We do not have an explanation for this effect. There was considerable hysteresis in the pressure–volume data of the high pressure phase on reducing the pressure, but not in the transition pressure nor in the low pressure phase.

The high-pressure phase was found to be slighty less compressible than determined by [7] over a more restricted pressure range (1–5 GPa). The volume data were fitted with a first-order Birch–Murnaghan equation of state [15], with V_0 and K_0 as the free parameters and the pressure derivative of the bulk modulus $K_0' = 4$. This equation of state was chosen because the limited pressure range investigated in this study prevents K_0' from being determined with sufficient accuracy and because the pressure steps taken here do not determine V_0 unequivocally. The agreement with the parameters determined from the data of [7] is reasonable (see table 1) and the major uncertainties are found to result from the poorly determined values of K_0'.

3.2. KOH

The spectra of KOH at ambient conditions were fitted with the structure determined previously (space group $P2_1/m$, [3]). The lattice parameters were calculated from a fit

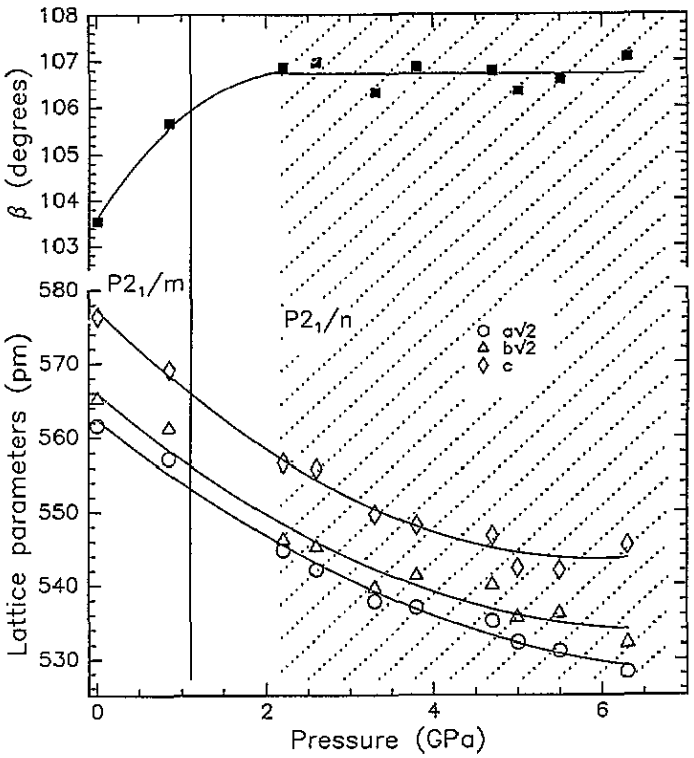

Figure 5. Lattice parameters of KOH in the low-pressure $P2_1/m$ and $P2_1/n$ structures. The transition between the two structures is of second order [3, 4]. The shaded area is the transition region between the $P2_1/n$ and the higher-pressure orthorhombic structure, the mid-point being indicated by a solid line (see figure 6).

to six lines, except 002 and 110 which overlap, and are in reasonable agreement with literature values (table 1). Raman and infrared studies [2] found a phase transition to a hydrogen-bonded phase at 0.7 GPa, and identified this as the low-temperature structure (space group $P2_1/n$). These two structures cannot be distinguished with x-ray methods [3, 4]. According to the latter studies, the phase transition is of second order. Figure 4 (bottom) shows an EDX spectrum of KOH at 2.8 GPa indexed in the $P2_1/m$ space group. The lattice parameters show a linear pressure dependence up to 2.6 GPa. However, there are not enough data points to confirm the second-order nature of this phase transition. With increasing pressure above the phase transition, there is a strong increase in the monoclinic angle β and the c lattice parameter (figure 5).

Between 6 and 7 GPa with increasing pressure, there is a phase transition to another high-pressure structure with a markedly different x-ray spectrum (figure 4, top). The transition region (marked by the upper and lower pressure limits of the observation of the low- and high-pressure phases, respectively) was bracketed by runs with increasing and decreasing pressure between 2 and 11 GPa (see figure 6). Optical studies [2] determined a range of coexistence from 4 to 7 GPa. The high-pressure structure can be indexed with an orthorhombic lattice. The small number of observed peaks and the presence of texture preclude a unique assignment of a space group. However, the anti-NaOH structure (space group *Pbcm*) gives a reasonable fit to the observed d-spacings and intensities (figure 4, top). The variation of the lattice parameters with pressure is shown in figure 6. The compression

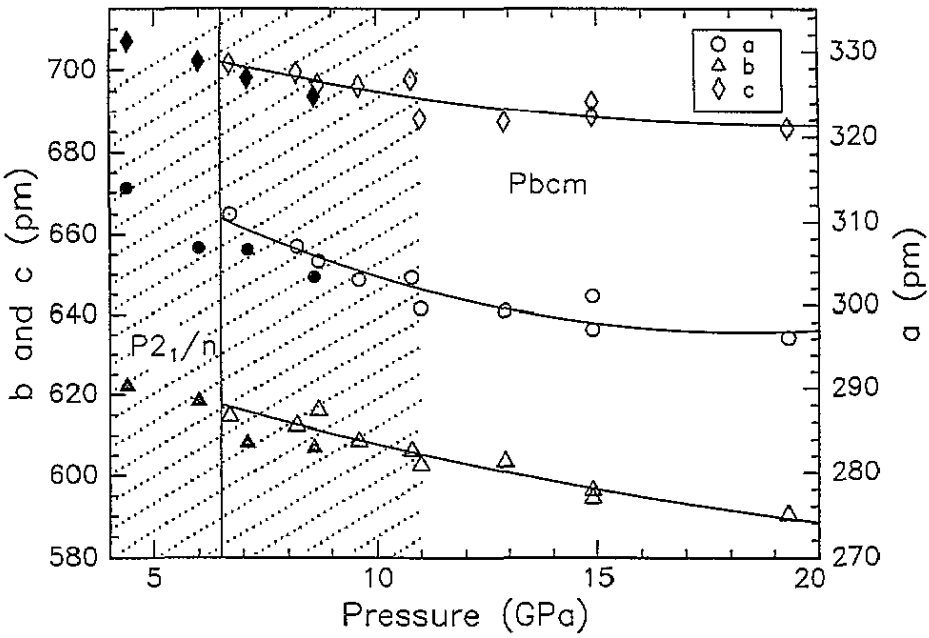

Figure 6. Lattice parameters of the high-pressure orthorhombic structure of KOH versus pressure, derived from indexing in the space group *Pbcm*. The shaded area represents part of the transition region to the lower pressure $P2_1/n$ structure (compare figures 5 and 7), the mid-point of this region being indicated by a solid line. The solid symbols represent runs with decreasing pressure. They were not used in the fits because the strong textures developed at the highest pressures create large uncertainties in the determination of the lattice parameters under these conditions.

is anisotropic, with the a and c lattice parameters showing a weaker pressure dependence.

The volume compressions of the different phases of KOH are shown in figure 7. A first-order Birch equation of state was fitted to the $P2_1/n$ phase. The parameters obtained are listed in table 1.

3.3. RbOH

For RbOH, no single-phase spectrum of the phase stable at ambient conditions was obtained on releasing the pressure from 1.3 and 1.7 GPa (this is above the phase transition to the intermediate-pressure phase at 1 GPa). The spectrum obtained at ambient conditions on pressure release consisted of a mixture of the ambient and intermediate pressure phases. The low-pressure structure was fitted with the structure determined previously for this phase (space group $P2_1/m$, [5]; table 1). The other phase corresponded to the low-temperature (or intermediate-pressure) structure (space group $Cmc2_1$; figure 8, bottom) with lattice parameters $a = 412.2(1)$, $b = 11.682$, $c = 423.6(1)$ pm. The volumes of the two coexisting phases are indistinguishable within the accuracy of the present method. The phase transition between the two phases takes place below 1.2 GPa, in agreement with [2] where a transition pressure of 0.8 GPa was determined (figure 9). Due to the lack of data below 1 GPa, the drop in the b lattice parameter at the phase transition cannot be determined. This would yield information about the change in the interlayer spacing. Neutron scattering experiments at different temperatures have determined a drop of 6% in b at the phase transition [5]. This change was explained by the break-up of the hydrogen bonds which link the metal–oxygen

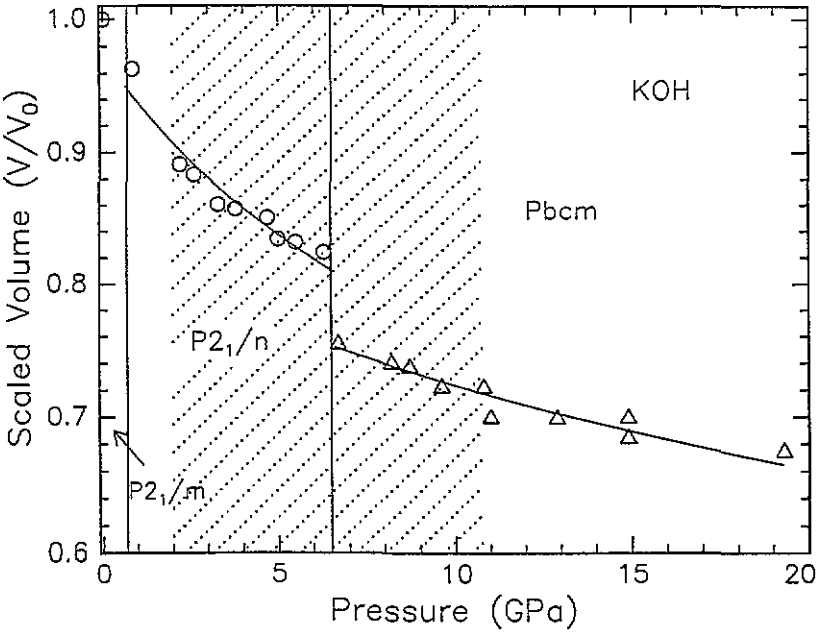

Figure 7. Scaled volume of the different phases of KOH versus pressure. The transition between the $P2_1/m$ and $P2_1/n$ structures is of second order. The shaded area represents the transition region between the $P2_1/n$ and the high-pressure *Pbcm* structures.

double layers [5].

In the $Cmc2_1$ phase, there is a linear decrease in the lattice parameters a and c, and a large, non-linear decrease in the b lattice parameter (figure 9). Similar phenomena have also been observed in the temperature-dependent studies [5] where the strong variation in b was interpreted as resulting from the gradual break-up of the hydrogen bonds.

A phase transition to another high-pressure phase was found between 5.6 and 7 GPa on increasing and between 4.2 and 3.1 GPa on decreasing pressure, in agreement with optical measurements [2] which determined an average pressure of 6.2 GPa for this transition. The EDX spectra of the high-pressure phase are remarkably similar to those of KOH in the high-pressure phase (compare figures 8 and 4, top). A fit with the anti-NaOH structure (space group *Pbcm*) with the same atomic position parameters as previously used for KOH yields reasonable intensities for most of the peaks (figure 8 and table 2). The Raman and infrared studies [2] had already concluded that the structures might be similar. However, the disagreement between the observed and calculated intensities of some peaks (notably 111, 131 and 211) suggests that the actual structure may be different from the one proposed here. The pressure dependence of the lattice parameters shows no anomaly (figure 10).

The volume compression of the different phases of RbOH is shown in figure 11; the equation of state parameters are listed in table 1.

3.4. CsOH

The lattice parameters of CsOH (table 1) were determined by a least-squares fit to at least four (and at most seven) of the following lines: (110), (021), (111), (130), (041), (002), (200), (112). The choice was constrained by the intensity of the peaks and overlap with fluorescence lines or their escape peaks. The spectra were indexed with the ambient-

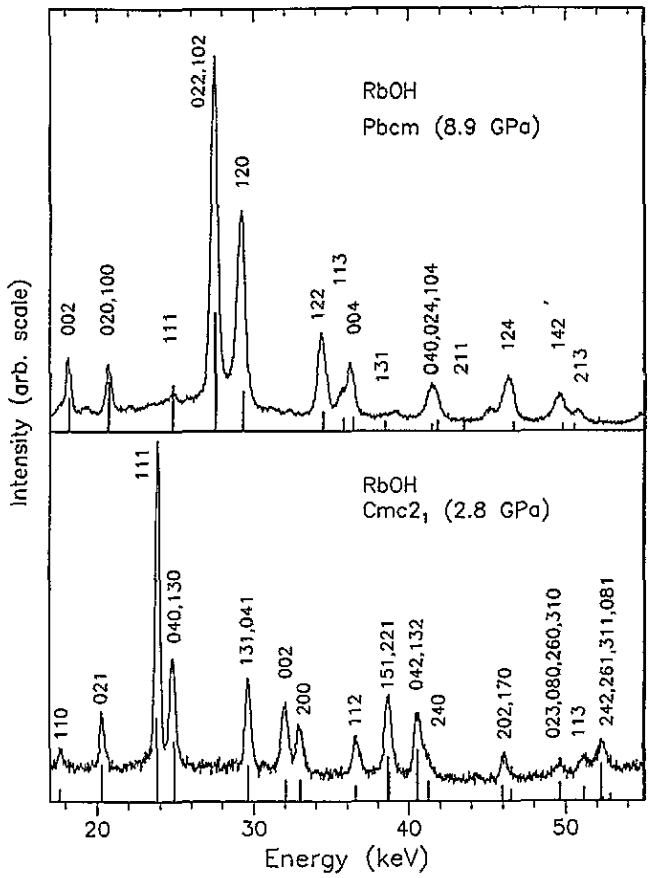

Figure 8. EDX spectra of RbOH at 2.8 GPa ($Cmc2_1$ structure, bottom) and at 8.9 GPa (top) at an angle of 5.38°. The high-pressure structure was indexed with, and intensities were calculated for, an anti-NaOH structure (space group *Pbcm*). Note the good overall agreement of the measured and calculated intensities, except for (111) and (211).

pressure structure (space group *Cmcm*) throughout the whole pressure range because it is indistinguishable by x-rays from the low-temperature $P2_12_12_1$ structure [6] (see figure 12 for an example at 9.6 GPa).

A phase transition from the room temperature *Cmcm* phase to the low-temperature structure (space group $P2_12_12_1$) was found by Raman and infrared measurements to take place between ambient conditions and 1 GPa at room temperature [2]. While the present data do not allow the different phases to be distinguished, there is a noticeable change in slope in the *b* lattice parameter above 1 GPa, suggesting that the phase transition does indeed lie below 1 GPa (figure 13). The phase transition between these two structures at ambient pressure as a function of temperature was found to be of second order, with changes in the slope of the *b* lattice parameter and in the volume as well as in the heat capacity c_p [6].

There is a strong decrease in the compressibility of the *b* and *c* lattice parameters with increasing pressure (figure 13). Actually, the slopes tend towards zero, and the *c* lattice parameter becomes similar to the *a* lattice parameter in the pressure range 11–15 GPa. This fact, together with the strong increase in the line width of certain lines above 10 GPa might be taken as evidence for an approach to a structural phase transition. However, the infrared

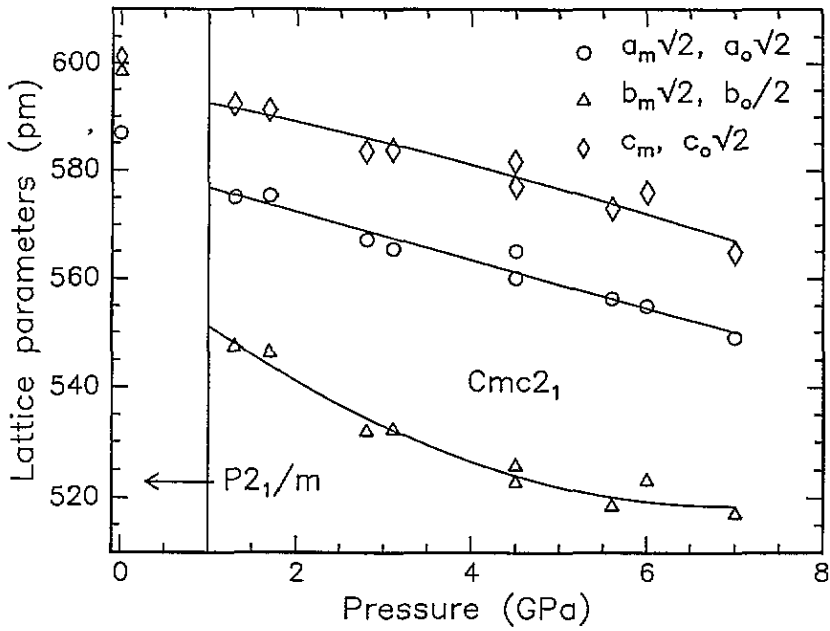

Figure 9. Lattice parameters of RbOH in the low-pressure $P2_1/m$ and $Cmc2_1$ structures. Note the non-linear compression of the *b*-axis perpendicular to the layers. The transition region between the $Cmc2_1$ and *Pbcm* structures is indicated on figures 10 and 11.

Table 2. Observed and calculated *d*-spacings and intensities of RbOH in the *Pbcm* structure at 8.9 GPa. The lattice parameters are $a = 320.6$ pm, $b = 637.1$ pm, $c = 727.1$ pm. The intensities were calculated for Rb in 4d with $x = 0.9$, O in 4c with $x = 0.42$, $y = 0.25$ using the ENDIX program [18].

	Observed		Calculated	
HKL	*d*-spacing (pm)	Intensity (%)	*d*-spacing (pm)	Intensity (%)
002	363.4	20	363.6	47
100			320.6	27
020	318.4	15	318.6	43
111	n.o.	n.o.	266.5	66
102			240.5	68
022	239.7	100	239.6	100
120	226.2	56	226.0	56
122	191.8	27	191.9	27
113	183.9	8	185.0	18
004	181.8	12	181.8	17
040	158.8	11	159.3	9
211	n.o.	n.o.	152.0	18
124	142.3	10	141.6	12
142	n.o.	n.o.	132.8	9
213	130.0	4	130.9	8
231	n.o.	n.o.	126.0	7

data do not show any evidence for a structural transition up to 25 GPa [2]. Raman studies show a strong increase in the frequency of the librational modes with pressure and hence

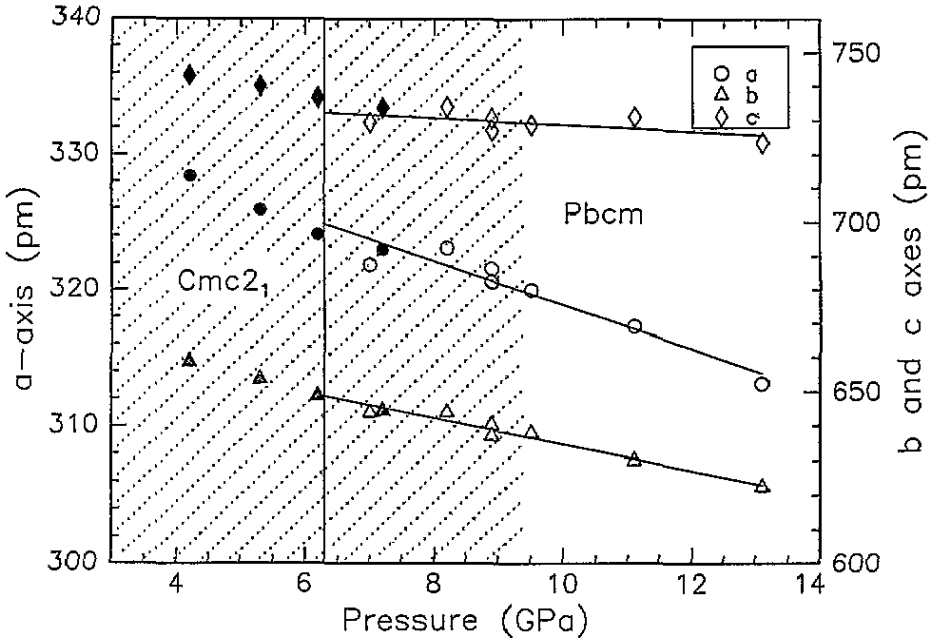

Figure 10. Lattice parameters of RbOH in the high-pressure orthorhombic structure, assuming the *Pbcm* space group. The transition region to the lower pressure $Cmc2_1$ structure is indicated by shading, the vertical line indicating the mid-point of this region. The hysteresis in the phase transition with decreasing pressure is shown by the solid symbols.

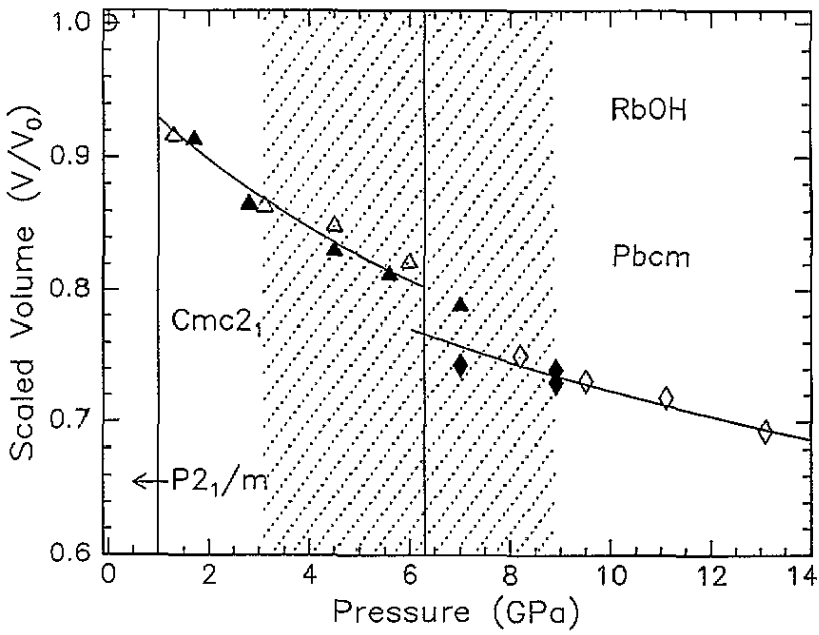

Figure 11. The scaled volume of RbOH in the three structures $P2_1/m$, $Cmc2_1$ and *Pbcm* versus pressure. The open and solid symbols represent two different runs.

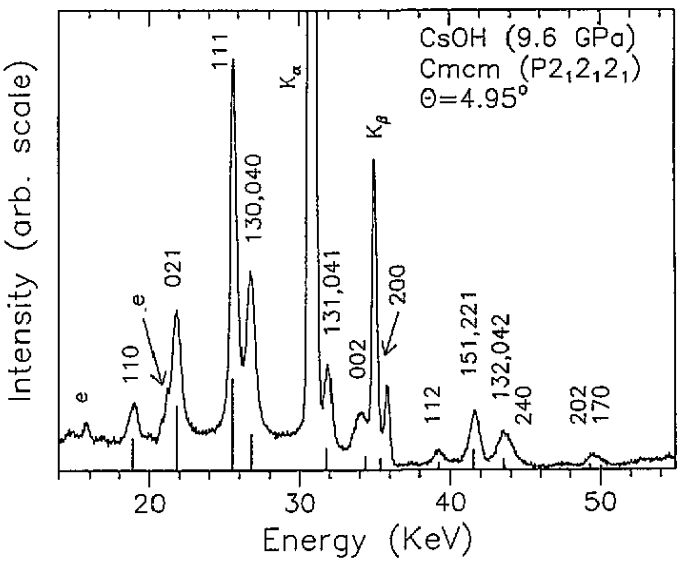

Figure 12. An EDX spectrum of CsOH at 9.6 GPa (*Cmcm* structure, indistinguishable from the true $P2_12_12_1$ structure). Intensities were calculated for the atomic positions determined at ambient conditions [8]. The sharp change in the background at 36 keV is due to a faulty field-effect transistor in the preamplifier of the detector. The asymmetry on the low-energy side of the (021) peak is due to overlap with two small escape peaks from the Cs Kα fluorescence.

an increasing strength of the hydrogen bonding [2].

The equation of state shows a smooth behaviour up to the highest pressure reached (figure 14 and table 2). Again, the pressure steps between the experiments are not small enough below 1 GPa to show evidence for a second-order phase transition.

4. Discussion

Earlier neutron and x-ray scattering studies [3–6, 14] have laid the basis for relating the changes in lattice parameters to the lattice dynamics of atomic and molecular motion. Together with the previous Raman and infrared measurements [1, 2], these studies also serve as the basis for interpreting the pressure dependence of the lattice parameters (at least at low pressures) since the behaviour with decreasing temperature and increasing pressure is closely analogous, and allows us to establish a partial systematics for this class of hydroxides.

The freezing-out of the motions of the OH^- groups with decreasing temperature from the high-temperature disordered NaCl to distorted NaCl-like structures leads to formation of metal–oxygen double layers. Formally, this occurs by sliding of (001) double layers in the [110] direction [14, 8]. Thus, in the monoclinic phases (generally $P2_1/m$), $c_m \geqslant a_c$, and $a_m \simeq b_m \simeq a_c/\sqrt{2}$ where $b_m \parallel [110]_c$ ($Z = 4$ in the NaCl structure while $Z = 2$ in the $P2_1/m$ structure). The protons in these phases (and in the disordered *Cmcm* phase of CsOH) hop between two potential minima [4–6]. With a further decrease in temperature, the protons become localized. The resulting reduction in their mutual repulsion (assisted by a sliding of layers in the monoclinic phases) leads to a decrease in the interlayer separation and formation of hydrogen bonds (except in NaOH). The resulting transitions to orthorhombic distorted TlI-type structures occur by a further sliding of the layers in the [110] direction [14, 8]. Thus, for the orthorhombic phases ($P2_12_12_1$, *Cmcm* and $Cmc2_1$), the relation

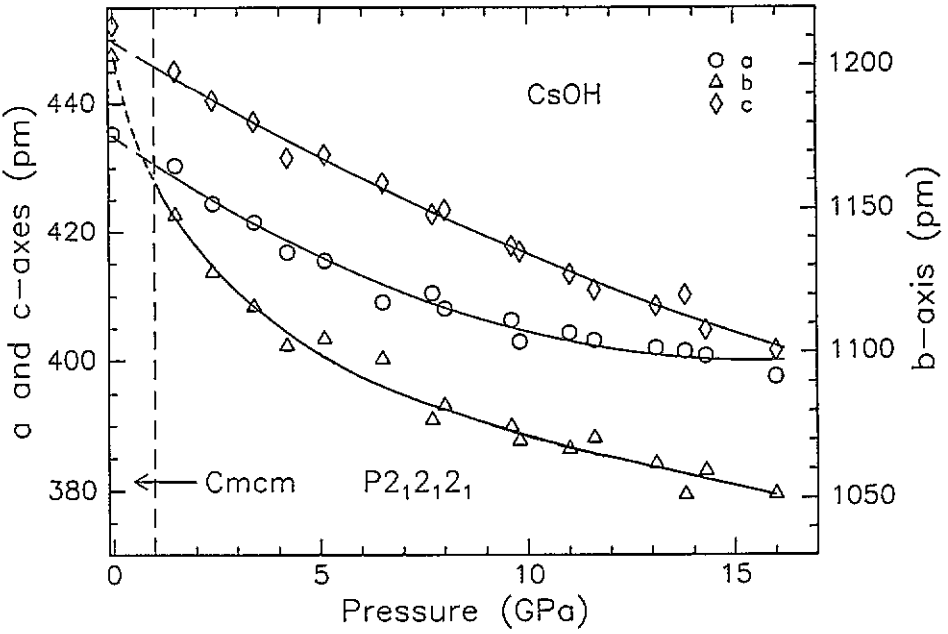

Figure 13. Lattice parameters of CsOH versus pressure. The data were fitted with the *Cmcm* space group throughout the whole pressure range since it cannot be distinguished from the $P2_12_12_1$ high-pressure structure. Note the strong curvature at high pressures in the a and b lattice parameters, and in the b lattice parameter at pressures around the phase transition. The lattice parameters a and c tend to become equal at high pressure. The line through the data points for the c lattice parameter is not a fit, but simply a guide to the eye.

between the orthorhombic and cubic lattice parameters is $b_o \simeq 2a_c$, and $a_o \simeq c_o \simeq a_c/\sqrt{2}$. The temperature range of sliding of layers and of strong changes in interlayer distances caused by the motion of the protons is marked by a strong temperature dependence of the monoclinic angle β (as in KOH and RbOH [4, 5]) and of the lattice parameter perpendicular to the maximum repulsion. In KOH and CsOH, these are the c_m and b_o axes, respectively, while the maximum repulsion in RbOH is not localized along any particular axis [4–6]. The present study shows that the behaviour with decreasing temperature and with increasing pressure is similar (see the changes in lattice parameters of KOH, RbOH and CsOH (figures 5, 9 and 13)).

At higher pressure, the phase transitions in NaOH, KOH and RbOH previously discovered [1, 2] lead to a phase which apparently is not layered (as was first shown for NaOH [7]). Interestingly, the transition takes place at a value of the lattice parameter perpendicular to the layers which is virtually identical for KOH and RbOH ($2c_m \sin\beta \simeq b_o \simeq 1040$ pm; figures 5, 9), and a little larger for NaOH (1080 pm, [7]). Note that the b lattice parameter for CsOH is around 1050 pm at 15 GPa, and that the a and c lattice parameters have become almost equal by that pressure (similar to the situation in NaOH at ambient conditions; see figure 13). This suggests that a phase transition to a *Pbcm*-like structure will take place also in CsOH at higher pressures. According to Raman and infrared studies [1, 2], the high-pressure phase of NaOH is not hydrogen bonded, in contrast to the corresponding phases of KOH and RbOH, and of LiOH [16]. Thus, it is quite possible that the structures of the high-pressure phases of NaOH, KOH and RbOH are not identical.

The compressibilities of NaOH and RbOH in the *Pbcm* structure are anisotropic, with

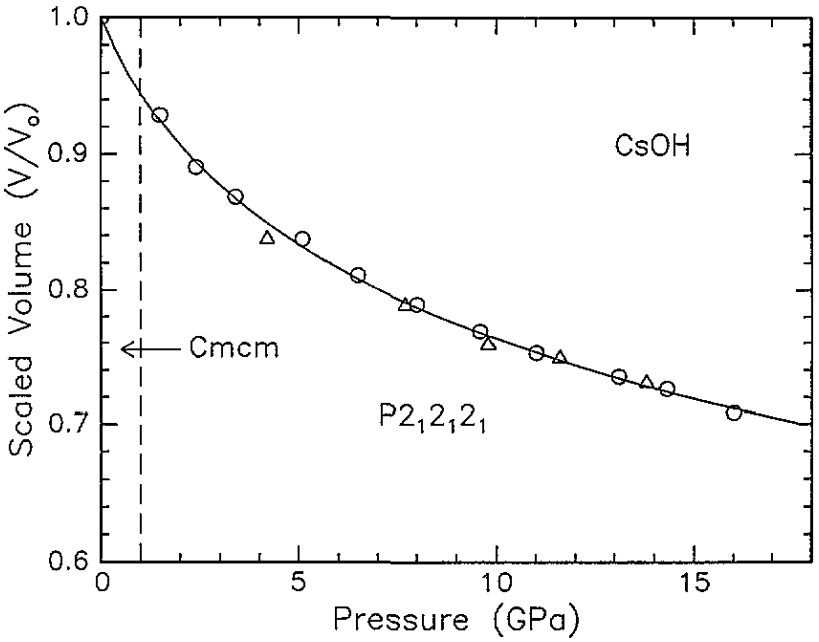

Figure 14. The scaled volume of CsOH versus pressure. The phase transition at around 1 GPa is of second order and the equation of state was fitted only to data above this pressure. The different symbols represent two different experiments.

the highest values being along the *b* direction. No such anisotropy was found in KOH.

The equation of state parameters determined here obviously suffer from the limited pressure range investigated, and from the lack of a precise determination of the volumes at the transition pressure in the case of KOH and RbOH. Thus, these values should be regarded only as parametrizations of the particular equation of state used. It was noted that runs with decreasing pressure in the *Pbcm* structure yielded pressure–volume data which showed strong deviations from the values determined on increasing pressure. This was not the case for the low-pressure structures. Hence, the former were not used in the determination of the equation of state parameters. The reason for this discrepancy may lie in the instability of the expanded gasket hole and the resulting pressure gradients on pressure release. The strong textures developed at the highest pressures reached created larger uncertainties in the determination of the lattice parameters on pressure release.

5. Final remarks

The structural systematics of the heavier alkali metal hydroxides (dominated by the layering at low pressure) continues into the higher-pressure regime. The high-pressure *Pbcm* structure according to [7] is a distorted variant of the NiAs structure. The present study suggests that this type of structure may be a common type of distortion from disordered structures in compounds with aspherical anions, in addition to the already well established case of distorted TlI-type structures [17]. It is somewhat surprising that no CsCl-type structure has been found to occur in the heavier alkali metal hydroxides at pressures up to 20 GPa. The transitions to the *Pbcm* structure in KOH and RbOH occur in the pressure range in which KCl and RbCl transform to the CsCl structure.

It is expected that the present study will stimulate more detailed investigations of the dynamics and the structures of the alkali metal hydroxides under pressure. In particular, the high-pressure structures of NaOH (at room temperature) and of KOH and RbOH (below room temperature) should be accessible to neutron studies with diamond anvil cells or with the recently developed large-volume cells (at room temperature) [19].

Acknowledgments

We thank H Barlage and Professor Jacobs (Uni Dortmund) for synthesis of CsOH and RbOH, and M Krobok for discussions on sample preparation. Financial support by the DFG is gratefully acknowledged.

References

[1] Krobok M P, Johannsen P G and Holzapfel W B 1992 *J. Phys.: Condens. Matter* **4** 8141
[2] Krobok M P, Johannsen P G and Holzapfel W B 1994 *J. Phys.: Condens. Matter* **6** 9789
[3] Jacobs H, Kockelkorn J and Tacke Th 1985 *Z. Anorg. Allg. Chem.* **531** 119
[4] Mach B, Jacobs H and Schäfer W 1987 *Z. Anorg. Allg. Chem.* **553** 187
[5] Jacobs H, Mach B, Lutz H-D and Henning J 1987 *Z. Anorg. Allg. Chem.* **544** 28
[6] Jacobs H, Mach B, Harbrecht B, Lutz H-D and Henning J 1987 *Z. Anorg. Allg. Chem.* **544** 55
[7] Beck H P and Lederer G 1993 *J. Chem. Phys.* **98** 7289
[8] Jacobs H and Harbrecht B 1981 *Z. Naturf.* b **86** 270
[9] Syassen K and Holzapfel W B 1975 *Europhys. Conf. Abstr.* **1A** 75
[10] Mao H K, Bell P M, Shaner J W and Steinberg D J 1978 *J. Appl. Phys.* **49** 3276
[11] Grosshans W A, Düsinger E-F and Holzapfel W B 1984 *High Temp.–High Pressures* **16** 539
[12] Otto J W 1993 *HASYLAB Jahresbericht* 931
[13] Pistorius C W F T 1969 *Z. Phys. Chem., NF* **65** 51
[14] Bleif H-J and Dachs H 1982 *Acta Crystallogr.* A **38** 470
[15] Birch F 1938 *J. Appl. Phys.* **9** 279
[16] Adams D A and Haines J 1991 *J. Phys. Chem.* **95** 7064
[17] Haines J and Christy A G 1992 *Phys. Rev.* B **46** 8797
[18] Hovestreydt E, Parthe E and Benedict U 1983 *J. Appl. Crystallogr.* **24** 282; 1987 *European Communities—Commission Report* EUR 10874, ECSC-EEC-EAEC, Brussels
[19] Besson J M, Pruzan Ph, Klotz S, Hamel G, Silvi B, Nelmes R J, Loveday J S, Wilson R M and Hull S 1994 *Phys. Rev.* B **49** 12559